

River Floodplains, Organic Carbon, and Paleoclimate: How River Dynamics Impart Biases in the Biogeochemical Climate Record of Terrestrial Landscapes

Authors:

Anjali M. Fernandes¹, Michael T. Hren², Virginia B. Smith³, Arvind Singh⁴, Dennis O. Terry Jr.⁵

¹Department of Earth and Environmental Sciences, Denison University, 100 W College Street, Granville, Ohio, 43023

²Department of Earth Sciences, University of Connecticut

³Department of Civil and Environmental Engineering, Villanova University, Philadelphia

⁴Arvind Singh, Department of Civil, Environmental and Construction Engineering, University of Central Florida, Orlando.

⁵Department of Earth and Environmental Science, Temple University

Corresponding author: Dr. Anjali M. Fernandes

Email: anjali.fernandes@denison.edu

Keywords: River dynamics, floodplains, particulate organic carbon, biomarkers, n-alkanes, terrestrial paleoclimate, hydroclimate, catchment hydrology, sediment flux, water flux

This is a non peer-reviewed pre-print submitted to EarthArXiv, and is currently in review at Frontiers in Earth Sciences.

Abstract

River floodplains can be both sources and sinks for organic carbon. In the sedimentary record, geochemical signatures of terrestrial water availability record climate and ecology along river corridors in deep time. However, paleoenvironmental reconstructions are often confounded by the complex dynamics of organic carbon residence, entrainment, and deposition in a fluvial system. As alluvial rivers migrate across their sedimentary basins, they erode older deposits, integrating their environmental record with that of other sediment in transport. Transported organic carbon deposited on floodplains integrates environmental information over spatiotemporal scales associated with sediment mobilized from the entire catchment. Carbon production from plant communities on stable floodplains contribute information about the local climate and ecology. If catchment-averaged, environmental signals may be integrated over more than $\sim 10^6$ years; if local, they may be integrated over just $\sim 10^4$ years. River dynamics therefore fundamentally impact the spatiotemporal scales of integration of environmental information encoded within the organic carbon stored on their floodplains.

We used physical experiments to explore how river kinematics impact the time over which organic carbon can accumulate on floodplain surfaces. We found that doubling the ratio of water to sediment flux caused the most stable parts of the floodplain to remain immobile for twice as long. In situ carbon accumulated on stable floodplains can therefore integrate significant amounts of local environmental information along with catchment-averaged information. Conversely, in situ organic carbon that accumulates on dynamic floodplains in systems with relatively high sediment fluxes predominantly records basin-averaged information but relatively small amounts of local information. Changes in river dynamics during past thermal events on Earth, linked to changes in the hydrological cycle and alterations in water and sediment fluxes, can be expected to alter the duration over which organic carbon can accumulate on Earth's river floodplains and therefore the spatial and temporal scales to which climate reconstructions apply.

Plain language summary

Along with the mineral sediment they transport (e.g., sand and mud), rivers also move organic carbon across continents and to oceans. Organic carbon particles can be stored in river sediment all along the river corridor, and then eventually remobilized. As a result, quantifying the time taken by carbon particles to move through the river network is challenging. In this work, we use experiments to explore how a changing climate might impact the rates at which carbon moves through rivers. We find that if a river

begins to carry more sediment than it used to, which is likely to happen as the Earth warms, the amount of time a carbon particle spends within the river network will be shortened.

1. Introduction

Rivers are sensitive gauges of environmental change, and their floodplains can serve as both sources and sinks for organic carbon. River channels erode, transport and deposit sediment as they build depositional landscapes, nourish ecological communities that rely on them, and fill terrestrial sedimentary basins. Organic carbon in alluvial sediment can provide students of Earth's climate history an abundance of information about the hydroclimate and ecological communities along river corridors and on floodplains in deep time (Wang et al., 2017). However, robust reconstructions of Earth's river landscapes and ecosystems hinge upon our ability to distinguish the potential spatial and temporal scales of integration of ecological information recovered from the deep time sedimentary record. Climate variability, and related changes in temperature and precipitation, can alter the kinematics of rivers and their floodplains by altering water and sediment fluxes. Terrestrial climate reconstructions rarely account for the impact of river dynamics on the recorded environmental information. Here, we use physical experiments of a distributive alluvial system to explore the role of channel and floodplain dynamics, influenced by differences in water and sediment flux, on the spatial heterogeneity in the environmental information recorded in fluvial deposits.

Leaf wax biomarkers, i.e., *n*-alkanes, in organic matter preserved in fluvial deposits can provide a quantitative record of past environments and climate variability. *n*-alkanes are waxes produced on the surface of plant leaves to aid in water repellency and shield against moisture loss (Holloway, 1969; Neinhuis and Barthlott, 1997). *n*-alkanes can be preserved over long timescales (Schimmelmann et al., 1997; Yang et al., 2011) and with minimal isotopic alteration. *n*-alkanes recovered from organic matter in fluvial deposits, if minimally degraded and abundantly preserved, provide 3 proxies for environmental change: (1) δD distributions of plant lipids, which are a function of climate, contain a time-integrated records precipitation δD (Sachse et al., 2012), (2) $\delta^{13}C$ isotopes of plants and their biomarkers can reflect ambient precipitation amount and physiological responses to moisture deficit or atmospheric pCO_2 (e.g., (Diefendorf et al., 2010), and (3) distribution of *n*-alkanes (Average Chain Length, ACL) in sediment changes dramatically as a function of environmental conditions and correlates well with atmospheric vapor pressure deficit (Eley and Hren, 2018). When *n*-alkanes are minimally degraded and abundantly preserved within sedimentary strata, δD , $\delta^{13}C$ and ACL data can provide a record of changing temperature and moisture deficit tied to global climatic change (Eley and Hren, 2018).

Organic matter present in sedimentary deposits (Fig. 1a) can be (a) detrital in origin, and carry catchment-integrated environmental information, or (b) deposited *in situ* and provide information about the local environmental conditions. If catchment-integrated, environmental signals may be integrated over millions of years, and represent spatial scales associated with the size of the catchment; if local, they may be integrated over just a few thousands of years, and represent much smaller spatial scales. Thus, the separation of local from catchment-integrated information has significant implications for the spatiotemporal scales over which paleoenvironmental reconstructions from biogeochemical proxies apply. By extension, this impacts the granularity with which climate perturbations with a range of (Fig. 1b). Parsing this information is possible with the depositional context provided by sedimentary facies. Organic matter is mostly abundant in floodplain sediments, and sampling floodplain sediments provide the best opportunity to ; however, not all floodplains are created equal. The organic carbon in young floodplain surfaces will be predominantly detrital or catchment-integrated; older floodplain surfaces will have accrued significantly more built-up *in situ* organic carbon containing a local environmental signal. Thus, floodplain age, and heterogeneity in floodplain ages, can significantly impact the fidelity of terrestrial paleoclimate reconstructions.

Over centuries or millennia, an alluvial river landscape (Fig. 1a) may be broadly differentiated into three regions: (1) the river channel, where deposits primarily store organic carbon and mineral detritus mobilized from the entire catchment upstream, (2) the active (proximal) floodplain, where deposited detrital sediment composition is gradually altered by weathering and local organic carbon from plant detritus accumulates in soils, and (3) the stable (distal) floodplain, where soil formation and the build-up of local organic carbon from plant matter dominates.

A laterally migrating river incorporates floodplain sediment into the transport system by bank erosion and leaves sediment behind in bars (Fig. 1a), thereby replacing a local climatic signal with a spatio-temporally integrated one. Rivers in alluvial basins build topographic relief because of higher rates of sediment deposition close to the channel (Fig. 1a). When the height of the water surface in the channel above the distal floodplain approaches one channel depth, the resulting hydraulic instability can cause a channel avulsion (Heller and Paola, 1996; Mohrig et al., 2000; Davies-Vollum and Kraus, 2001; Slingerland and Smith, 2004). Flow finds a new path at a lower elevation on the floodplain, where it may re-occupy an older abandoned channel or form a new channel (Hajek and Edmonds, 2014; Chamberlin and Hajek, 2015; Edmonds et al., 2016). If the newly avulsed channel erodes floodplain sediment, the stored (local) signal will be replaced by a spatially- and temporally-averaged signal in the carbon record.

Thus, if the rates of *in situ* organic debris accumulation remain equal, a river system that migrates rapidly and avulses frequently will primarily accumulate inherited, catchment-integrated environmental

information and the age of local carbon will be small; a less dynamic system in which floodplains remain stable for longer periods of time will accumulate more *in situ* environmental information and the age of local carbon will be larger. We therefore hypothesize that river dynamics, influenced by the ratio of water flux to sediment flux, impact (a) the residence time of *in situ* organic carbon in floodplains, and (b) the temporal and spatial integration of environmental information recovered from floodplain sediment.

We use an experimental distributive fan system to evaluate how differences in the ratio of water discharge to sediment discharge can impact: (1) landscape stability, and (2) spatial heterogeneity in floodplain age, and use our finding to draw inferences about the associated carbon residence times and biases in paleoclimate reconstructions from the biogeochemical proxy record.

2. Experimental Conditions

We used two physical experiments, performed at Tulane University (Wang et al., 2011; Straub and Wang, 2013), to evaluate how the kinematics of the transport system influence floodplain stability. In these experiments, a fan delta evolved freely under two sets of steady boundary conditions. We used these datasets to evaluate the influence of the ratio of water discharge to sediment discharge on floodplain stability, and therefore the potential heterogeneity in the recovered biomarker record.

The experiments were performed in an experimental basin that was 0.65 m deep, and measured 4.2 m and 2.8 m in the downstream and cross-stream directions respectively (Wang et al., 2011; Straub and Wang, 2013). A mixture of silica, crushed coal and water was released into the experimental basin at a constant rate and under the influence of gravity. The water in the mixture was dyed blue. In physical experiments such as these, unrealistic geometric scales (high ratios of particle size to flow depths, steep transport slopes, etc.) compared to natural systems are ignored as long as a range of transport styles, i.e. from bedload to suspended load, are observed (Paola et al., 2009). The sediment mixture, composed of a 3:7 volumetric ratio of crushed coal (S.G. = 1.3; $D_{50} = 440\mu\text{m}$) and higher density silica (S.G. = 2.65; $D_{50} = 110\mu\text{m}$), allowed for a full spectrum of transport styles, from bedload to suspended load, in these experiments. Built by shallow channels with steep longitudinal profiles, the experimental deltas used herein do not display any influence from a backwater effect on channel dynamics e.g., (Te Chow, 1959; Paola and Mohrig, 1996; Nittrouer et al., 2012; Fernandes et al., 2016; Ganti and Chadwick, 2016; Martin et al., 2018). The observed dynamics are therefore most relevant to fan deltas (e.g., (Nemec and Steel, 1988)) or distributive fluvial systems (e.g., (Hartley et al., 2010)).

Prior to the start of each experiment, sediment deposition built a prograding subaerial platform while base-level was maintained at a constant elevation; the experiment began once this initial platform was built. For the duration of each experiment, water supply, sediment supply and base-level rise rate (pseudo-subsidence) were held constant (Table 1). The fixed rate at which accommodation was generated through base-level rise was matched against the fixed rate at which sediment was supplied such that the shoreline position did not change for the duration of each experiment. This stationarity precludes any potential influence that shoreline progradation or regression, equivalent to facies belt migration at the field-scale (Hickson et al., 2005), may have on the measured dynamics and organization in the transport system. In Experiments 1 and 2, the same base-level rise rate was used, but the ratio of water to sediment supplied to the basin in Experiment 2 was twice that of Experiment 1 (Table 1).

<i>Table 1: Boundary conditions associated with the physical experiments</i>		
Experiment	Experiment 1 (TDB-10-1)	Experiment 2 (TDB-11-1)
Water Flux : Sediment Flux Qw:Qs	1x 0.451 L/s : 0.011 L/s	2x 0.902 L/s : 0.011 L/s
Base-level rise rate	5mm/h	5mm / h
Duration of data-set used here	1000 min	1000 min

3. Data and Methods

We used sequential, orthorectified overhead images that represent 1000 timesteps (1000 minutes of experimental time) from each experiment, we mapped the location and relative depth of flow through time across the surface of each experiment. We applied two thresholds to the blue luminosity pixel values in these overhead images, using a methodology implemented in a number of previous studies (e.g. (Li et al., 2016; Scheidt et al., 2016)). The two thresholds were set and verified using visual inspection (Fig. 2), and then used to separate dry portions of the experiment (without blue dye) from locations inundated by shallow flow (small values of blue luminosity) and deeper, channelized flow (larger values of blue luminosity).

We use deep, channelized flow as representative of river channels in field-scale fluvial systems; shallow, sheet flow represents overbank flow in active floodplains; dry areas of the experimental surface

represent stable floodplain (Fig. 1a, 2). Channelized flow and sheet flow in similar fan delta experiments have been shown to be associated with periods of sediment erosion and storage, respectively (Sheets et al., 2002). During periods of sediment erosion or downstream flushing, the area of the surface that is occupied by deeper flow in channels increases. Over time, sediment is flushed through the system and deposited at the downstream termini of channels, reducing the longitudinal channel gradient (Kim et al., 2014). The resulting decrease in sediment transport capacity causes channel filling, lateral flow expansion and widespread inundation by sheet flow. Periods of inundation by sheet flow are tied to widespread deposition and a steepening of the longitudinal gradient.

In each experiment, we used one cross-stream transect at which cumulative deposition between the inlet and the transect accounted for approximately 60% of the sediment mass (Straub and Wang, 2013). At each pixel, we created a time-series to identify the presence of dry floodplain, channelized flow or sheet flow at each pixel along the transect (Fig. 2). Next, we generated distributions to quantify the fraction of the chosen transect that was occupied by each landscape state at each time-step (Fig. 3, a b). We then quantified the temporal persistence of each landscape state, i.e., floodplain (Fig. 3c, d), sheet flow (Fig. 3e, f), and channelized flow (Fig. 3g, h). For example, when a pixel transitioned from wet (channelized flow or sheet flow) to dry floodplain, we counted the number of time-steps (experiment minutes) for which it remained dry before converting back to a wet surface.

Finally, we generated a comparative assessment of the impact of a difference in the ratio of water to sediment flux on the heterogeneity in floodplain age across a landscape transect at a given time (Fig. 4). To assess the potential variability encountered along the geomorphic surface at any given time, such as at 1000 minutes for example (Fig. 4 a, b), we used the calculated ages of floodplain surfaces for all 1000 time steps (Fig. 4 c, d) to generate cumulative frequency distributions of instantaneous floodplain ages for each time-step and all time-steps together (Fig. 4 e, f), and exceedance probabilities for the floodplain surface ages encountered on a geomorphic surface at any time (Fig. 4, g, h).

Results

The fraction of the selected transects occupied by floodplain, sheet flow and channelized flow (Fig. 3 a, b) are not significantly different between experiments. As indicated by the 25th, 50th and 75th percentiles, denoted hereafter by p25, p50 and p75 respectively, floodplains generally occupied a slightly larger fraction of the transect in Experiment 1 (p25 = 0.4, p50 = 0.5, p75 = 0.6) than in Experiment 2 (p25 = 0.33, p50 = 0.42, p75 = 0.52; Fig. 3 a,b). Sheet flow generally covered a larger fraction of the transect

than channelized flow in both experiments; sheet flow occupied a smaller fraction of the transect in Experiment 1 ($p_{25} = 0.28$, $p_{50} = 0.35$, $p_{75} = 0.43$) than in Experiment 2 ($p_{25} = 0.3$, $p_{50} = 0.4$, $p_{75} = 0.5$), whereas channelized flow generally occupied a similar fraction in Experiment 1 ($p_{25} = 0.08$, $p_{50} = 0.14$, $p_{75} = 0.20$) and Experiment 2 ($p_{25} = 0.13$, $p_{50} = 0.15$, $p_{75} = 0.2$).

There were significant differences in the persistence of floodplains, sheet flow and channelized flow in the two experiments; all categories were generally more persistent in Experiment 2. Notably, doubling the ratio of water flux to sediment flux resulted in floodplain stability timescales (Fig. 3 c, d) that were roughly twice in Experiment 2 ($p_{50} = 10$ minutes, $p_{95} = 96$ minutes) than in Experiment 1 ($p_{50} = 5$ minutes, $p_{95} = 48$ minutes). Sheet flow stability timescales in Experiment 1 ($p_{50} = 5$ minutes, $p_{95} = 18$ minutes) were smaller than in Experiment 2 ($p_{50} = 6$ minutes, $p_{95} = 33$ minutes); similarly, stability timescales of channelized flow in Experiment 1 ($p_{50} = 4$ minutes, $p_{95} = 14$ minutes) were smaller than in Experiment 2 ($p_{50} = 6$ minutes, $p_{95} = 25$ minutes). The number of measurements “n” in Figures 4 c - h, hold information about the fraction of the transect occupied by floodplain, sheet flow and channelized flow, as well as the mobility of each category; however, since the fraction of the transects occupied by each category were not significantly different between experiments, lower “n” values signify fewer measurements and therefore greater stability.

A visual assessment of Figure 4 a- d suggests that while floodplain extent, lateral continuity and frequency of occurrence in time are greater in Experiment 1, floodplain surfaces are generally young. This is internally consistent with the number of measurements ($n = 13,126$) in Figures 3c and 3d, as well as the smaller flow stability timescales in Figures 3e and 3g. Conversely, floodplain surfaces tend to be spaced farther apart in time, are less continuous laterally and can be significantly older in Experiment 2; this assessment is supported by the smaller number of measurements in Figure 3d, and the larger flow stability timescales in Figures 3f and 3h. Importantly, instantaneous floodplain ages on geomorphic surfaces, quantified in Figures 4e & 4f, highlight that higher ratios of water to sediment fluxes in Experiment 2 generate floodplains ages ($p_{50} = 20$ minutes, $p_{95} = 100$ minutes) that are generally twice that in Experiment 1 ($p_{50} = 40$ minutes, $p_{95} = 100$ minutes). The exceedance probability calculations of floodplain age show power laws with higher slopes in Experiment 1 than in Experiment 2 (Fig. 4, g & h); the exceedance probability of encountering a floodplain surface with an age of 100 minutes is an order of magnitude higher in Experiment 2 than Experiment 1.

Discussion

Our results indicate that the morphodynamics of alluvial rivers, a function of sediment and water supply, can significantly impact the residence times of particulate organic carbon in Earth's floodplains and bias reconstructions of paleoclimate and paleotopography (Tipple et al., n.d.; Pagani et al., 2006; Hren et al., 2010; Feakins et al., 2012; Hren and Ouimet, 2021; Chang et al., 2023). Furthermore, although we specifically evaluate climate proxies tied to organic carbon in floodplains, our findings are relevant to any terrestrial climate proxies connected to timescales of floodplain stability (e.g., soil carbonates, geochemical climofunctions, etc.).

Comparing results from these experiments, we see that reduced relative sediment loads in Experiment 2, i.e., larger ratios of water flux to sediment flux ($Q_w:Q_s$), decreased the lateral mobility of flow. Associated floodplain surfaces showed significantly more spatial heterogeneity in surface age and the oldest floodplain surfaces remained stable for twice as long relative to the oldest floodplain surfaces in Experiment 1. We can therefore infer that biomarkers recovered from floodplains with greater stability are more likely to deliver paleoclimate reconstructions with temporal and spatial granularity that is commensurate with an *in situ*, unmixed environmental signal. However, the characteristic timescale associated with a significant build-up of local particulate organic carbon debris, a function of local hydroclimate, must be accounted for. For instance, an alluvial system in which the exceedance probability of floodplain age is twice that of the characteristic timescale required to generate a clear *in situ* environmental signal may be expected to produce a record of local paleoenvironmental states at higher spatial and temporal resolution than one in which the two timescales are comparable.

Biomarkers recovered from channel deposits or young floodplain surfaces, on the other hand, can be expected to provide a catchment-integrated estimate of hydroclimate with far less spatio-temporal granularity. Dynamic floodplain surfaces with greater spatial homogeneity in age, associated with alluvial systems in which smaller ratios of water to sediment flux like Experiment 1, are more likely to be biased towards storing a catchment integrated record of paleoclimate. The spatial footprint of environmental reconstructions from channel deposits or young floodplains would likely scale with the size of the catchment; the temporal footprint would be similar to the median age of carbon exported from the catchment.

Modern rivers display a latitudinal gradient in the ages of exported carbon (Eglinton et al., 2021); high latitude rivers transport carbon with the greatest range in ages and largest ages. Climate models forecast an invigoration of the Earth's hydrological cycle as the planet warms; changing precipitation patterns that result are likely to drive changes in the ratios of water flux to sediment flux through rivers. In un-engineered rivers that are allowed to migrate laterally, changes in lateral migration rates should be

expected to produce differences in the range in the age of particulate organic carbon transported by rivers. Similarly, changes in river dynamics during thermal events in Earth's past, linked to changes in the hydrological cycle and alterations in water and sediment fluxes, should be expected to have altered carbon residence times in Earth's river systems. These alterations, and associated biases in terrestrial climate reconstructions, must be accounted for when reconstructing environmental conditions from floodplain POC. It is therefore essential to integrate biogeochemical proxy reconstructions with qualitative and quantitative information about sedimentary processes (e.g. floodplain stability and weathering, channel mobility, estimates of water and sediment fluxes, etc.), to assess the spatial and temporal scales to which paleoclimate reconstructions apply.

Acknowledgements

This work was supported by funding from the National Science Foundation grants EAR-2023710 and EAR-2029803. The authors thank the Tulane Sediment Dynamics and Stratigraphy group and the Sediment Experimentalists Network for the collection and archival of data.

References

- Chamberlin, E. P., and Hajek, E. A. (2015). Interpreting paleo-avulsion dynamics from multistory sand bodies. *Journal of Sedimentary*. Available at: <https://pubs.geoscienceworld.org/sepm/jsedres/article-abstract/85/2/82/145463>.
- Chang, Q., Hren, M. T., Lai, L. S.-H., Dorsey, R. J., and Byrne, T. B. (2023). Rapid topographic growth of the Taiwan orogen since ~1.3-1.5 Ma. *Sci. Adv.* 9, eade6415.
- Davies-Vollum, K. S., and Kraus, M. J. (2001). A relationship between alluvial backswamps and avulsion cycles: an example from the Willwood Formation of the Bighorn Basin, Wyoming. *Sediment. Geol.* Available at: <https://www.sciencedirect.com/science/article/pii/S003707380000186X>.
- Diefendorf, A. F., Mueller, K. E., Wing, S. L., Koch, P. L., and Freeman, K. H. (2010). Global patterns in leaf ^{13}C discrimination and implications for studies of past and future climate. *Proc. Natl. Acad. Sci. U. S. A.* 107, 5738–5743.
- Edmonds, D. A., Hajek, E. A., Downton, N., and Bryk, A. B. (2016). Avulsion flow-path selection on rivers in foreland basins. *Geology* 44, 695–698.
- Eley, Y. L., and Hren, M. T. (2018). Reconstructing vapor pressure deficit from leaf wax lipid molecular distributions. *Sci. Rep.* 8, 3967.
- Feakins, S. J., Warny, S., and Lee, J.-E. (2012). Hydrologic cycling over Antarctica during the middle Miocene warming. *Nat. Geosci.* 5, 557–560.

- Fernandes, A. M., Törnqvist, T. E., and Straub, K. M. (2016). Connecting the backwater hydraulics of coastal rivers to fluvio-deltaic sedimentology and stratigraphy. Available at: <https://pubs.geoscienceworld.org/gsa/geology/article-abstract/44/12/979/195074>.
- Ganti, V., and Chadwick, A. J. (2016). Avulsion cycles and their stratigraphic signature on an experimental backwater-controlled delta. *Journal of*. Available at: <https://agupubs.onlinelibrary.wiley.com/doi/abs/10.1002/2016JF003915>.
- Hajek, E. A., and Edmonds, D. A. (2014). Is river avulsion style controlled by floodplain morphodynamics? *Geology*. Available at: <http://geology.gsapubs.org/content/42/3/199.short>.
- Hartley, A. J., Weissmann, G. S., Nichols, G. J., and Warwick, G. L. (2010). Large Distributive Fluvial Systems: Characteristics, Distribution, and Controls on Development. *J. Sediment. Res.* 80, 167–183.
- Heller, P. L., and Paola, C. (1996). Downstream changes in alluvial architecture; an exploration of controls on channel-stacking patterns. *J. Sediment. Res.* Available at: <https://pubs.geoscienceworld.org/sepm/jsedres/article-abstract/66/2/297/113942>.
- Hickson, T. A., Sheets, B. A., Paola, C., and Kelberer, M. (2005). Experimental Test of Tectonic Controls on Three-Dimensional Alluvial Facies Architecture. *J. Sediment. Res.* 75, 710–722.
- Holloway, P. J. (1969). The effects of superficial wax on leaf wettability. *Ann. Appl. Biol.* 63, 145–153.
- Hren, M. T., and Ouimet, W. (2021). Organic Molecular Paleohypsometry: A New Approach to Quantifying Paleotopography and Paleorelief. *Front Earth Sci. Chin.* 9. doi: 10.3389/feart.2021.665324.
- Hren, M. T., Pagani, M., Erwin, D. M., and Brandon, M. (2010). Biomarker reconstruction of the early Eocene paleotopography and paleoclimate of the northern Sierra Nevada. *Geology* 38, 7–10.
- Kim, W., Petter, A., Straub, K., and Mohrig, D. (2014). “Investigating the autogenic process response to allogenic forcing: experimental geomorphology and stratigraphy,” in *From Depositional Systems to Sedimentary Successions on the Norwegian Continental Margin*, eds. A. W. Martinus, R. Ravnås, J. A. Howell, R. J. Steel, and J. P. Wonham (Chichester, UK: John Wiley & Sons, Ltd), 127–138.
- Li, Q., Yu, L., and Straub, K. M. (2016). Storage thresholds for relative sea-level signals in the stratigraphic record. *Geology*. Available at: <https://pubs.geoscienceworld.org/gsa/geology/article-abstract/44/3/179/131999>.
- Martin, J., Fernandes, A. M., Pickering, J., Howes, N., Mann, S., and McNeil, K. (2018). The Stratigraphically Preserved Signature of Persistent Backwater Dynamics in a Large Paleodelta System: The Mungaroo Formation, North West Shelf, Australia. *J. Sediment. Res.* 88, 850–872.
- Mohrig, D., Heller, P. L., Paola, C., and Lyons, W. J. (2000). Interpreting avulsion process from ancient alluvial sequences: Guadalope-Matarranya system (northern Spain) and Wasatch Formation (western Colorado). *GSA Bulletin* 112, 1787–1803.
- Neinhuis, C., and Barthlott, W. (1997). Characterization and Distribution of Water-repellent, Self-cleaning Plant Surfaces. *Ann. Bot.* 79, 667–677.
- Nemec, W., and Steel, R. J. (1988). What is a fan delta and how do we recognize it. *Fan Deltas: sedimentology and tectonic settings* 3, 231–248.

- Nittrouer, J. A., Shaw, J., Lamb, M. P., and Mohrig, D. (2012). Spatial and temporal trends for water-flow velocity and bed-material sediment transport in the lower Mississippi River. *Bull. Am. Assoc. Hist. Nurs.* Available at: <https://pubs.geoscienceworld.org/gsa/gsabulletin/article-abstract/124/3-4/400/125770>.
- Pagani, M., Pedentchouk, N., Huber, M., Sluijs, A., Schouten, S., Brinkhuis, H., et al. (2006). Arctic hydrology during global warming at the Palaeocene/Eocene thermal maximum. *Nature* 442, 671–675.
- Paola, C., and Mohrig, D. (1996). Palaeohydraulics revisited: palaeoslope estimation in coarse-grained braided rivers. *Basin Res.* 8, 243–254.
- Paola, C., Straub, K., Mohrig, D., and Reinhardt, L. (2009). The “unreasonable effectiveness” of stratigraphic and geomorphic experiments. *Earth-Sci. Rev.* Available at: <https://www.sciencedirect.com/science/article/pii/S001282520900083X>.
- Sachse, D., Billault, I., Bowen, G. J., Chikaraishi, Y., Dawson, T. E., Feakins, S. J., et al. (2012). Molecular Paleohydrology: Interpreting the Hydrogen-Isotopic Composition of Lipid Biomarkers from Photosynthesizing Organisms. doi: 10.1146/annurev-earth-042711-105535.
- Scheidt, C., Fernandes, A. M., and Paola, C. (2016). Quantifying natural delta variability using a multiple-point geostatistics prior uncertainty model. *J. Geophys. Res.* Available at: <http://onlinelibrary.wiley.com/doi/10.1002/2016JF003922/full>.
- Schimmelmann, A., Lange, C. B., Zhao, M., and Harvey, C. (1997). Southern California’s megaflood event of ca. 1605 AD linked to large-scale atmospheric forcing.
- Sheets, B. A., Hickson, T. A., and Paola, C. (2002). Assembling the stratigraphic record: depositional patterns and time-scales in an experimental alluvial basin. *Basin Res.* 14, 287–301.
- Slingerland, R., and Smith, N. D. (2004). RIVER AVULSIONS AND THEIR DEPOSITS. *Annu. Rev. Earth Planet. Sci.* 32, 257–285.
- Straub, K. M., and Wang, Y. (2013). Influence of water and sediment supply on the long-term evolution of alluvial fans and deltas: Statistical characterization of basin-filling sedimentation patterns. *J. Geophys. Res. Earth Surf.* 118, 1602–1616.
- Te Chow, V. (1959). *Open-channel hydraulics*. McGraw-Hill New York.
- Tipple, B. J., Meyers, S. R., and Pagani, M. (n.d.). Carbon isotope ratio of Cenozoic CO₂: A comparative evaluation of available geochemical proxies. *Paleoceanography*. doi: 10.1029/2009PA001851.
- Wang, C., Eley, Y., Oakes, A., and Hren, M. (2017). Hydrogen isotope and molecular alteration of n-alkanes during heating in open and closed systems. *Org. Geochem.* 112, 47–58.
- Wang, Y., Straub, K. M., and Hajek, E. A. (2011). Scale-dependent compensational stacking: An estimate of autogenic time scales in channelized sedimentary deposits. *Geology* 39, 811–814.
- Yang, H., Liu, W., Leng, Q., Hren, M. T., and Pagani, M. (2011). Variation in n-alkane δD values from terrestrial plants at high latitude: Implications for paleoclimate reconstruction. *Org. Geochem.* 42, 283–288.

Figures

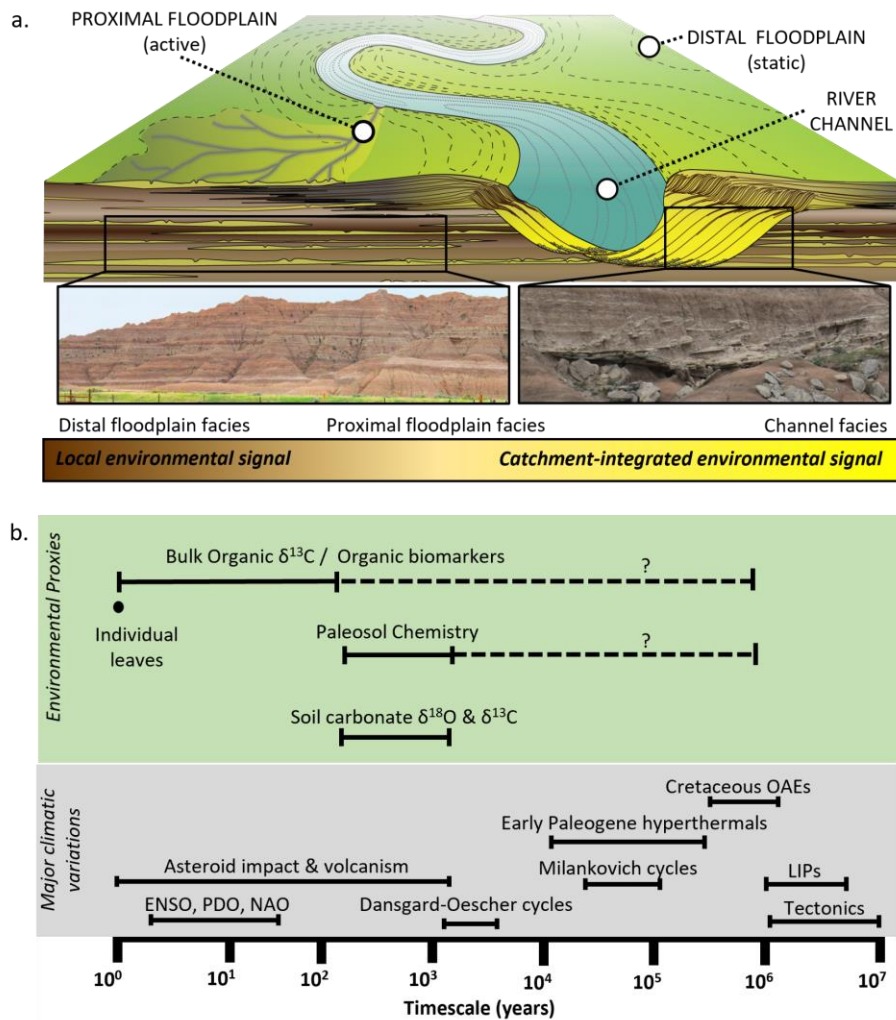


Figure 1: (a) An illustration showing sedimentary facies that provide environmental context for the spatial and temporal scales of integration associated with the biogeochemical climate proxies they hold.

(b) Representative time scales of major modern climatic variations, and past geologic events are compared to the estimated time scales of integration associated with different climate proxies.

Abbreviations: ENSO = El Niño Southern Oscillation; PDO = Pacific Decadal Oscillation; NAO = North Atlantic Oscillation; OAEs = ocean anoxia events; LIPs = large igneous provinces. Solid range bars correlate with assumptions of in situ information whereas dashed bars correlate with the potential temporal scales of integration when the environmental signal is catchment-integrated.

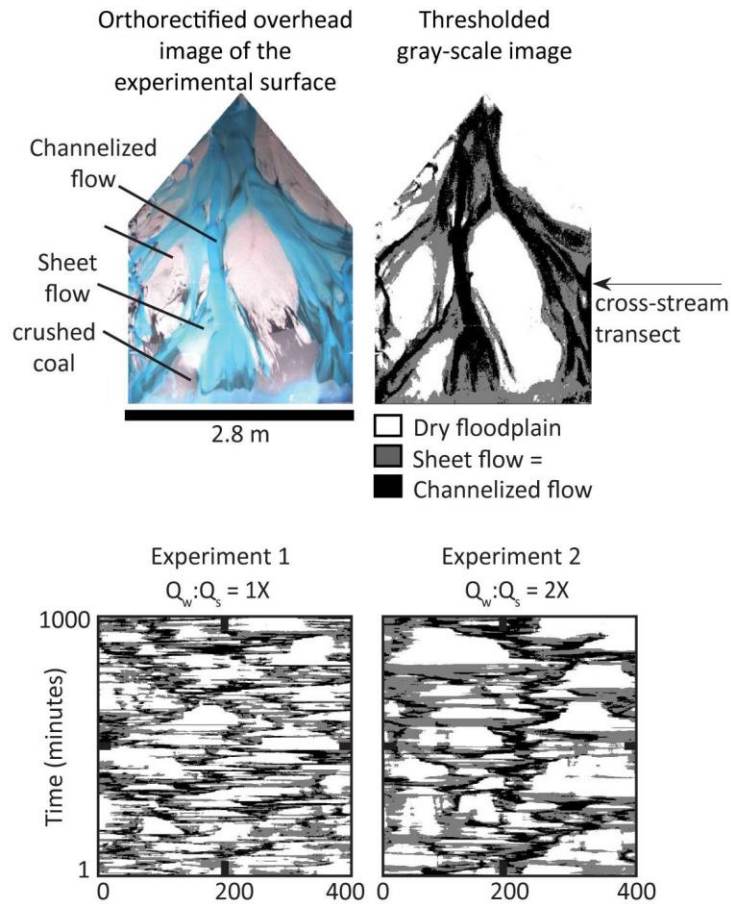


Figure 2: Methodology applied to 1000 sequential orthorectified images from each experiment. (A) Orthorectified overhead full-color RGB images. (B) Thresholded gray-scale images where white pixels represent dry floodplain, grey pixels represent shallow sheet flow, and black pixels represent deep, channelized flow. (C) Time-space matrices of stacked, thresholded pixel values at a cross stream transect.

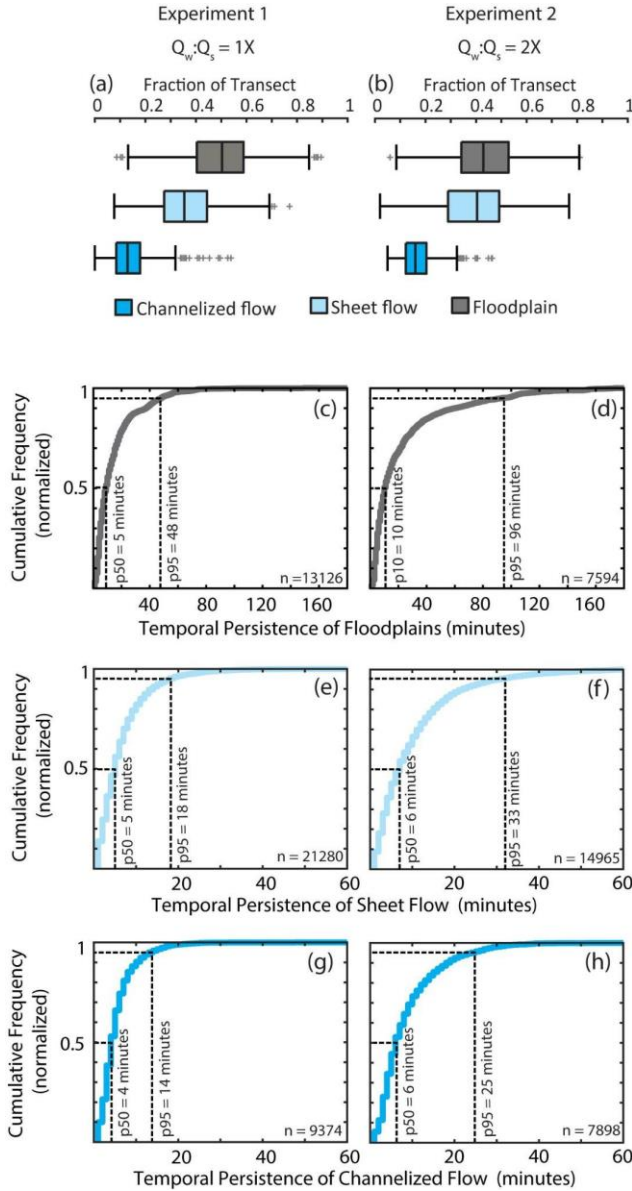


Figure3: Box and whisker plots showing the distribution in the fraction of the transect covered by floodplain, sheet flow and channelized flow at all 1000 time-steps in Experiment 1 (a) and Experiment 2 (b). The vertical bar at the center of the box represents the 50th percentile of values, the upper and lower bounds on the boxes represent the 25th and 75th percentiles respectively, and the upper and lower bounds on the whiskers represent the 10th and 90th percentile respectively. Normalized cumulative frequencies quantify temporal persistence of (c), (d) stable floodplain, (e), (f) sheet flow and (g), (h) channelized flow in Experiment 1 (left) and Experiment 2 (right) respectively.

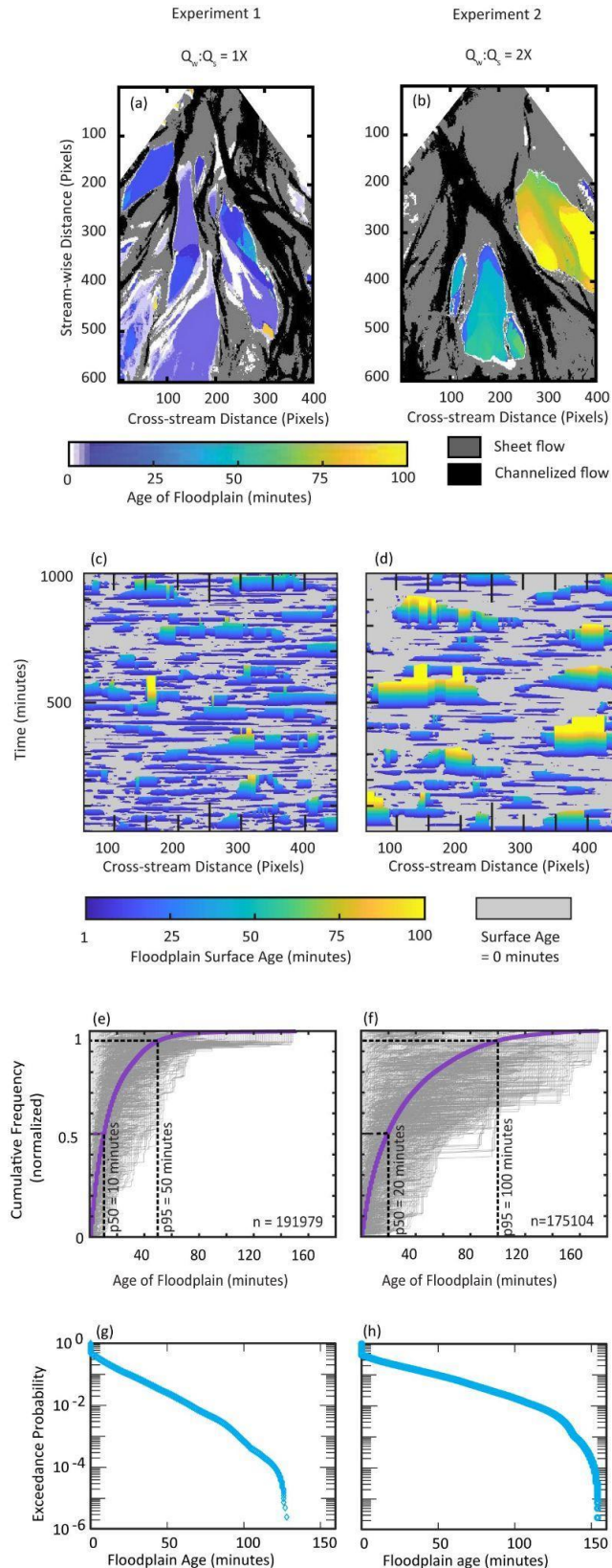


Figure 4: Examples of floodplain ages mapped onto the dry areas of the experimental surface at one “snapshot” in time (1000 minutes) in Experiments 1 (a) and 2 (b). Time-space matrices showing floodplain surfaces and their age, encountered at any given time-step at a cross-stream transect in Experiments 1 (c) and 2 (d). Normalized cumulative frequency distributions of the ages of all floodplains encountered at the surface at each time-step (pale grey) and at all timesteps (bold magenta) along the same transect in Experiments 1 (e) and 2 (f), respectively. Exceedance probabilities associated with floodplains of different ages in Experiments 1 (g) and 2 (h).